

## Intrinsic optical anisotropy of quantum wells in cubic crystals

E. G. Tsitsishvili\*

*Institut für Angewandte Physik, Universität Karlsruhe, D-76128 Karlsruhe, Germany*

(Received 18 January 1995; revised manuscript received 18 April 1995)

The intrinsic optical anisotropy of flat quantum wells (QW's) grown from cubic materials is investigated on the basis of an envelope-function approximation. It is shown that optical polarization effects in (11*N*)-oriented QW's are caused by the warping of the hole energy spectrum, and that they are the more pronounced the stronger the anisotropy of hole effective masses is. An analytic dependence of the optical matrix elements on the thickness of the QW's is found. Qualitative estimates of the intrinsic optical anisotropy for (100)-oriented QW's in GaAs and AlAs are given.

### I. INTRODUCTION

In recent years, optical polarization effects in semiconductor microstructures have been discovered. In particular, the optical anisotropy in flat quantum wells and superlattices was observed in the luminescence,<sup>1-3</sup> the photocurrent,<sup>4</sup> and the reflection spectra.<sup>5</sup>

The strong polarization anisotropy of the excitonic luminescence excitation spectra has been attributed to the corrugation of heteroboundaries.<sup>2,3</sup> The essential argument in the above claims is the increase of the anisotropy effects, with the decrease of the quantum well (QW) thickness.

On the other hand, it is obvious that the optical response of the confined media is nonlocal.<sup>6</sup> As a result, the QW's must exhibit intrinsic optical anisotropy. It is known that the optical properties of the two-dimensional structures are different in the growth direction and in a plane of the layer.<sup>7</sup> In addition, the phenomenological treatment shows that the optical constants in the cubic QW's oriented along the crystal directions other than (111) and (100) depend on the direction of the polarization of light in the plane of the QW. Therefore, the QW's grown in the crystal directions of low symmetry exhibit not only in-plane (for light propagating along the plane of the well), but also transversal (for light propagating in the growth direction) anisotropic optical effects.

In Ref. 8, numerical calculations of the intrinsic in-plane optical anisotropy (IOA) for GaAs/AlAs QW's were given. The well-width dependence of optical anisotropy was attributed to the presence of the split-off state. In reality, there is obviously a coexistence of the IOA and the anisotropy due to technological reasons such as surface corrugations. Therefore, it is important to theoretically investigate the possible microscopic mechanisms responsible for the IOA, and to estimate quantitatively the effects anticipated. In the present paper, the results of an analytic calculation of the IOA in (11*N*)-oriented cubic QW's are reported. This is, to our knowledge, the first report on the analytic investigation of the IOA in dependence of the well thickness and orientation.

### II. THEORY

We consider an isolated quantum well grown in a [11*N*] direction, which we take as the quantization axis *z*. Hence, the axis *z* is oriented along [11*N*], the *x* axis is oriented along [1 $\bar{1}$ 0], and the *y* axis is oriented along [001] (for *N*=0), [11 $\bar{2}$ ] (for *N*=1), [11 $\bar{1}$ ] (for *N*=2), [33 $\bar{2}$ ] (for *N*=3), etc.

We analyze QW's with direct dipole allowed interband transitions. The resonance part of the dielectric tensor  $\epsilon_{ij}(\omega)$  is given by the expression

$$\epsilon_{ij}(\omega) \sim \sum_{v,n,m,\vec{k}_\perp} \frac{(P_i^v)_{nm}(P_j^v)}{\hbar\omega - E_n(k_\perp) + E_{mv}(\vec{k}_\perp) + i\gamma} \Bigg|_{\gamma \rightarrow 0}, \quad (1)$$

where  $\vec{P}_{nm}^v$  is the matrix element of the momentum operator  $\hat{P}$ :

$$(P_i^v)_{nm} = \langle nc | e_i \hat{P}_i | mv \rangle, \quad (2)$$

where the unit vector  $\vec{e}$  coincides with the direction of the light polarization.

In Eqs. (1), (2), the index *i* = 1lh, 2lh, 1hh, 2hh designate the bands of light and heavy holes, index *c* corresponds to the conduction band, *n* and *m* are quantum numbers of electrons and holes. The functions  $|mv\rangle$  and  $|nc\rangle$  are the hole and the electron wave functions at the Brillouin-zone center at the point  $\vec{k}_\perp = 0$  ( $|\vec{k}_\perp| = \sqrt{k_x^2 + k_y^2}$ ). The energies  $E_{n,mv}(\vec{k}_\perp)$  are the electron and hole energies of the conduction and valence subbands, respectively.

For light linearly polarized parallel to the plane of the QW, the anisotropy of the transversal components of the dielectric tensor  $\epsilon_{xx}$  and  $\epsilon_{yy}$  leads to the intrinsic optical anisotropy in the QW's, i.e., to the linear anisotropic optical spectra of absorption and reflection, as well as to the intrinsic birefringence. On the other hand, Eq. (1) shows that the anisotropy of the dielectric tensor is a consequence of the polarization dependence of the interband optical transitions. Therefore, the anisotropy of the matrix elements is responsible for the intrinsic anisotropic

optical effects in QW's.

In the framework of the effective-mass approximation,<sup>9</sup> electronic states are the products of the envelope function in the  $z$  direction and the basic functions of the bulk crystals. For the conduction band  $\Gamma_6$  the basic functions  $|S\rangle$  have  $s$ -like symmetry. Thus, the electron wave functions  $|nc\rangle$  are given by the expression

$$|nc\rangle = |S\rangle \varphi_s f_n(z). \quad (3)$$

The hole basic function,  $|\vec{J}, j\rangle$ , coincide with the eigenfunctions of the operator of the total momentum  $\vec{J} = \vec{l} + \vec{s}$  and its projection  $j$ . In the  $|\vec{J}, j\rangle$  basis, the spin-orbit interaction Hamiltonian matrix is diagonal, and the valence bands  $\Gamma_8$  and  $\Gamma_7$  are completely split at the  $\Gamma$  point. For  $\vec{k} \neq 0$ , the  $\Gamma_8$  and  $\Gamma_7$  states are mixed depending on the ratio of the hole kinetic energy and the spin-orbit splitting  $\Delta_{so}$ . In the case of QW, the mixing of  $\Gamma_8$  and  $\Gamma_7$  states is governed by the ratio of the hole quantization energy and the energy difference between the  $\Gamma_8$  and  $\Gamma_7$  subbands. Therefore, this ratio depends on the QW

thickness. We shall assume that the splitting  $\Delta_{so}$  is large compared to the quantization energy  $\epsilon_q$  and treat the  $\Gamma_8 - \Gamma_7$  mixing by perturbation theory. We use a type of the perturbation theory described by Löwdin<sup>10</sup> and calculate the size corrections for the simple model of QW with the infinitely high potential barrier.<sup>11</sup> In other words, we assume that the potential barrier  $V$  is much larger than the quantization energy  $\epsilon_q$  and the penetration into the barrier can be neglected for a first approximation. Evidently, the first condition ( $\Delta_{so} \gg \epsilon_q$ ) is stronger if the potential barrier is large compared to the spin-orbit splitting, while the second condition ( $V \gg \epsilon_q$ ) is stronger in the opposite case ( $\Delta_{so} > V$ ). In our approximation, the electron wave function  $f_n(z)$  is given by

$$f_n(z) = \sqrt{2/L} \sin \left[ n\pi \frac{z}{L} \right], \quad n = 1, 2, \dots, \quad (4)$$

where  $L$  is the QW thickness. At the Brillouin-zone center, the  $6 \times 6$  matrix of the Luttinger Hamiltonian for  $[11N]$ -oriented QW's in the  $|J, j\rangle$  basis can be written as

$$H = -\epsilon_m \begin{pmatrix} P+Q & L & M & 0 & i\frac{L}{\sqrt{2}} & -i\sqrt{2}M \\ L^* & P-Q & 0 & M & -i\sqrt{2}Q & i\sqrt{3/2}L \\ M^* & 0 & P-Q & -L & -i\sqrt{3/2}L^* & -i\sqrt{2}Q \\ 0 & M^* & -L^* & P+Q & -i\sqrt{2}M^* & -i\frac{L^*}{\sqrt{2}} \\ -i\frac{L^*}{2} & i\sqrt{2}Q & i\sqrt{3/2}L & i\sqrt{2}M & -\Delta+P & 0 \\ i\sqrt{2}M^* & -i\sqrt{3/2}L^* & i\sqrt{2}Q & i\frac{L}{\sqrt{2}} & 0 & -\Delta+P \end{pmatrix}, \quad (5)$$

where

$$\epsilon_m = \frac{\hbar^2 K_m^2}{2m_0}, \quad K_m = m\pi/L, \quad m = 1, 2, \dots, \quad (6)$$

and

$$\Delta = \frac{\Delta_{so}}{\epsilon_m} \quad (7)$$

In Eq. (5), the functions  $P$ ,  $Q$ ,  $L$ , and  $M$  are equal to

$$\begin{aligned} P &= \gamma_1, \quad Q = 2\gamma_2(\frac{3}{2}\cos^2\chi - 1), \\ L &= \sqrt{\frac{3}{2}}\gamma_3(1-i)\sin 2\chi, \end{aligned} \quad (8)$$

$$M = \sqrt{3}i\gamma_3\cos^2\chi,$$

$\chi$  being the angle between the  $z$  axis and the crystal direction  $[110]$ . In Eq. (8),  $\gamma_1$ ,  $\gamma_2$ , and  $\gamma_3$  are the Luttinger parameters.

Because of the mixing of the hole basic states, the hole wave functions  $|mv\rangle$  in the first order on the  $\Gamma_8 - \Gamma_7$  in-

teraction are given by

$$\begin{aligned} |mv\rangle &= \sum_{j=\pm 1/2, \pm 3/2} a_j^v \left[ \left| \frac{3}{2}, j \right\rangle \right. \\ &\quad \left. + \sum_{s=\pm 1/2} \frac{H_{|3/2, j\rangle, |1/2, s\rangle}}{\Delta} \right. \\ &\quad \left. \times \left| \frac{1}{2}, s \right\rangle \right] \sin(K_m z). \end{aligned} \quad (9)$$

The basis functions  $|\vec{J}, j\rangle$  can be expressed in terms of the space functions  $X$ ,  $Y$ , and  $Z$  and the spin functions  $\alpha$  and  $\beta$ :

$$\begin{aligned}
|\frac{3}{2}, \frac{3}{2}\rangle &= \frac{1}{2} \{ (1-i)[Z \cos\chi - Y \sin\chi] + (1+i)X \} \alpha, \\
|\frac{3}{2}, \frac{1}{2}\rangle &= \frac{i}{2\sqrt{3}} \{ (1-i)[Z \cos\chi - Y \sin\chi] \beta + (1+i)X \beta \\
&\quad - 2\sqrt{2}[Y \cos\chi + Z \sin\chi] \alpha \}, \\
|\frac{3}{2}, -\frac{1}{2}\rangle &= \frac{1}{2\sqrt{3}} \{ (1+i)[Z \cos\chi - Y \sin\chi] \alpha + (1-i)X \alpha \\
&\quad + 2\sqrt{2}[Y \cos\chi + Z \sin\chi] \beta \}, \\
|\frac{3}{2}, -\frac{3}{2}\rangle &= \frac{i}{2} \{ (1+i)[Z \cos\chi - Y \sin\chi] + (1-i)X \} \beta, \\
|\frac{1}{2}, \frac{1}{2}\rangle &= \frac{1}{\sqrt{6}} \{ (1-i)[Z \cos\chi - Y \sin\chi] \beta + (1+i)X \beta \\
&\quad + \sqrt{2}[Y \cos\chi + Z \sin\chi] \alpha \}, \\
|\frac{1}{2}, -\frac{1}{2}\rangle &= \frac{i}{\sqrt{6}} \{ (1+i)[Y \sin\chi - Z \cos\chi] \alpha - (1-i)X \alpha \\
&\quad + \sqrt{2}[Y \cos\chi + Z \sin\chi] \beta \}.
\end{aligned} \tag{10}$$

$$A^2 = 1/2\delta(Q + \delta),$$

and

$$\delta(\chi) = \sqrt{\gamma_2^2(\cos^4\chi + 4\sin^4\chi - \sin^2 2\chi) + 3\gamma_3^2(\cos^4\chi + \sin^2 2\chi)}.$$

We consider two first interband transitions from heavy-hole and light-hole subbands with quantum number  $m=1$  to the conduction subband with  $n=1$ , and calculate the following relative quantities:

$$\delta_{\text{lh, hh}} = \frac{|P_X^{l,h}|^2 - |P_Y^{l,h}|^2}{|P_Y^{l,h}|^2}, \tag{13}$$

where

$$|P_{X,Y}^{l,h}|^2 = |P_{X,Y}^{1l,1h}|^2 + |P_{X,Y}^{2l,2h}|^2. \tag{14}$$

The quantities  $\delta_{\text{lh}}$  and  $\delta_{\text{hh}}$  describe the degree of the optical anisotropy. Thus, according to the relation (1), they determine the normalized intensities of the differential optical spectra, related with the contributions of the optical transitions from the light- and heavy-hole subbands, respectively.

By inserting Eqs. (4) and (9)–(11) into Eq. (2) the matrix elements are calculated. The quantities  $\delta_{\text{lh}}$  and  $\delta_{\text{hh}}$  are found to be

$$\begin{aligned}
\delta_{\text{lh}} &= \frac{3(\gamma_2 - \gamma_3)}{2} \left[ \frac{1}{\gamma_+(\chi)} + \frac{\delta(\chi)}{3\Delta(\chi)} [2\Delta(\chi) + 1] \right. \\
&\quad \left. \times \frac{\hbar^2 \pi^2}{2m_0 L^2 \Delta_{\text{so}}} \right] a(\chi),
\end{aligned} \tag{15}$$

and

$$\begin{aligned}
\delta_{\text{hh}} &= \frac{3(\gamma_3 - \gamma_2)}{2} \left[ \frac{1}{\gamma_-(\chi)} + \frac{\delta(\chi)}{3\Delta(\chi)} [2\Delta(\chi) - 1] \right. \\
&\quad \left. \times \frac{\hbar^2 \pi^2}{2m_0 L^2 \Delta_{\text{so}}} \right] a(\chi),
\end{aligned}$$

The coefficients  $a_j^p$  are defined by

$$\{a^{1\text{lh}}\} = \begin{bmatrix} Q + \delta \\ L^* \\ M^* \\ 0 \end{bmatrix} A, \quad \{a^{2\text{lh}}\} = \begin{bmatrix} 0 \\ M \\ -L \\ Q + \delta \end{bmatrix} A, \tag{11}$$

$$\{a^{1\text{hh}}\} = \begin{bmatrix} -L \\ Q + \delta \\ 0 \\ -M \end{bmatrix} A, \quad \{a^{2\text{hh}}\} = \begin{bmatrix} -M \\ 0 \\ Q + \delta \\ L^* \end{bmatrix} A,$$

where

where the function  $\delta(\chi)$  is determined by the Eq. (12) and the function  $a(\chi)$  is equal to

$$a(\chi) = \cos^2\chi(1 - 3\sin^2\chi). \tag{16}$$

The other functions in Eq. (12) are given by the expressions:

$$\begin{aligned}
\gamma_{\pm}(\chi) &= \delta(\chi) \pm \Delta(\chi), \\
\Delta(\chi) &= \gamma_2\beta(\chi) + \gamma_3\gamma(\chi), \\
\beta(\chi) &= (\frac{3}{2}\cos^2\chi - 1)(1 - 3\cos^2\chi), \\
\gamma(\chi) &= -\frac{2}{3}\sin^2 2\chi.
\end{aligned} \tag{17}$$

In the particular case of  $\chi=0$  and large well thickness  $L$ , these results coincide with those found by Kajikawa, Hata, and Isu.<sup>12</sup>

### III. DISCUSSION

Our analytic results [Eq. (15)] enable us to make the conclusions on the intrinsic optical anisotropy in [11N]-oriented QW's grown from cubic materials. In this section, we discuss the theoretical results and give their comparison with the known experimental data.

(i) First of all, note that the in-plane optical matrix elements are isotropic in (100)- and (111)-oriented QW's. Indeed, the function  $a(\chi)$  in Eq. (16) is equal to zero at  $\chi=\pi/2$  and  $\chi=\arcsin(1/\sqrt{3})$ . In the other (11N)-oriented QW's, the interband optical matrix elements are anisotropic, depending on the direction of the light polarization in the plane of the QW. This optical anisotropy is

caused by the nonanalyticity of the hole wave functions in the vicinity of the center of the Brillouin zone, and, as a consequence, by the mixing of light- and heavy-hole states. The anisotropy vanishes if the zone-center Luttinger Hamiltonian is diagonal [as for (100)-oriented QW's], or if the hole states mixing is independent of the hole mass parameters  $\gamma_2$  and  $\gamma_3$  [as for (111)-oriented QW's]. Note, that a similar mechanism is responsible for the optical anisotropy in bulk crystals with spatial dispersion.<sup>13</sup>

As follows from Eq. (15), the difference between the matrix elements corresponding to two perpendicular polarization of light (along axes  $x$  and  $y$ ) is proportional to the difference of the material parameters ( $\gamma_2 - \gamma_3$ ). In a bulk crystal, this constant difference is responsible for the warping of the hole energy spectrum in the  $\Gamma_8$  valence band.

(ii) It may be seen from Eqs. (15) that the quantities  $\delta_{lh}$  and  $\delta_{hh}$  have opposite sign.<sup>14</sup> This means that the polarizations of the peak values of the heavy-hole exciton and light-hole exciton are opposite to each other in the optical spectra: one peak is strengthened for  $X$  (or  $Y$ ) polarization, while the other is emphasized for  $Y$  (or  $X$ ) polarization.<sup>15</sup> The sign of  $\delta_{lh}$  and  $\delta_{hh}$  is changed at an angle  $\chi$  around  $35^\circ$ . And so, the (110)-oriented QW and, for example, the (113)-oriented QW showed the opposite behavior.

(iii) The first term in Eq. (15) describes the contribution of the  $\Gamma_8$  states and defines the optical anisotropy in the wide QW's, where the mixing of the  $\Gamma_{8-}$  and  $\Gamma_{7-}$  states can be neglected. In addition, this term does not depend on the height of the potential barrier at all. This is important, since it enables us to calculate the minimum relative anisotropy exactly. From Eq. (15) follows also that for QW's grown from the same materials, the optical anisotropy has its maximum value for the (110) orientation. Indeed, the dependence on the well orientation is described basically by the function  $a(\chi)$ .<sup>14</sup> The function  $a(\chi)$  is defined by the Eq. (16) and given in the inset of the Fig. 1. It may be seen that it is maximal at  $\chi=0$ .

As an example, the optical anisotropy in the wide QW's grown from GaAs is given in Fig. 1. Figure 1 shows the functions  $\delta_{lh}$  and  $\delta_{hh}$  in dependence of the direction of the quantization axes. The following value of the band parameters were used:  $\gamma_2=2.1$  and  $\gamma_3=2.9$ . It may be seen that the optical anisotropy in (110)-oriented GaAs QW reaches the value 0.17 for  $\delta_{hh}$  and  $(-0.34)$  for  $\delta_{lh}$ . The anisotropy for the 1hh-1c transitions has a maximum for the (110) polarization and a minimum for the (100) polarization, while for the 1lh-1c transitions the anisotropy shows the opposite polarization dependence. The optical anisotropy is smaller in QW's oriented along directions other than [110]. In [112]- and [113]-oriented QW's the quantities  $\delta_{lh}$  and  $\delta_{hh}$  change their sign.

(iv) The second term in Eq. (15) is related with the spin-orbit split valence band  $\Gamma_7$ . It may be seen, that the mixing of the  $\Gamma_8$  and  $\Gamma_7$  states leads to the dependence of the optical anisotropy on the well thickness  $L$ . The anisotropy increases with decreasing thickness as  $1/L^2$ . Such a dependence on the well size is a consequence of

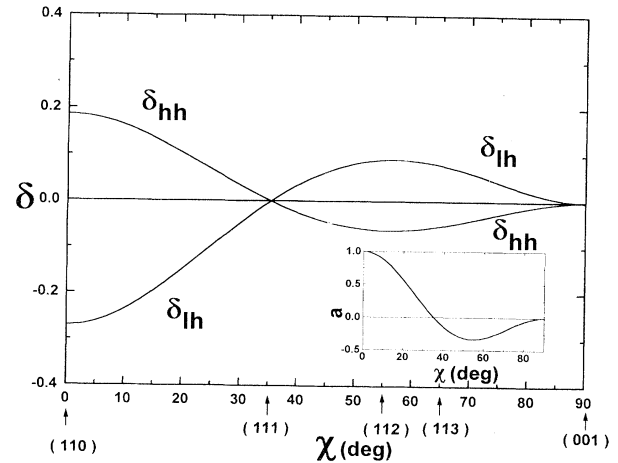


FIG. 1. The in-plane anisotropy  $\delta$ , as a function of the angle  $\chi$  between the quantization axis  $z$  and crystal direction [110].  $\delta$  is defined by Eq. (15). The designations hh and lh indicate the heavy- and light-hole subbands. The inset shows the function  $a(\chi)$  vs the angle  $\chi$ . The function  $a(\chi)$  is defined by the Eq. (16).

the approximation used: the large spin-orbit splitting and infinitely high potential barrier. In this case, the mixing of the  $\Gamma_8$  and  $\Gamma_7$  states is treated as a perturbation and the quantization energy is proportional to the  $1/L^2$ . The well size region where this approximation is valid depends on the specific structure of the QW's.

The finite potential barrier quantum well can be considered as an infinitely high potential barrier QW, with an effective thickness  $\tilde{L}$  wider than the geometric size  $L$  of the QW. Then, the Eq. (15) preserves its form with the replacement of the  $L$  by the  $\tilde{L}$ , and, therefore, the size

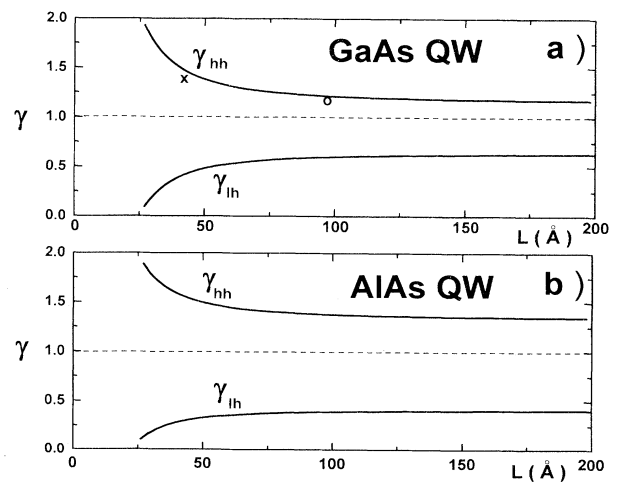


FIG. 2. The in-plane anisotropy  $\gamma = \delta + 1$  as a function of the well width  $L$  for [110]-oriented GaAs QW (a) and AlAs QW (b).  $\delta$  is defined by Eq. (15). The designations hh and lh indicate the heavy and light valence subbands. The cross and open circle are experimental data points from Refs. 1 and 4.

TABLE I. The quantities  $\delta_{lh}$  and  $\delta_{hh}$  in dependence of the well thickness  $L$ . In the columns (Ref. 1), (Ref. 4), and (Ref. 5) the experimental data by Gershoni *et al.*, Kajikawa *et al.*, and Belousov *et al.*, respectively, are given. The columns (Ref. 8) and (Ref. 8)<sup>†</sup> contain the results of the numerical calculations by Nojima for GaAs/Al<sub>0.7</sub>Ga<sub>0.3</sub>As QW's and for GaAs/AlAs QW's (indicated by the dagger †). In the column (Cal.), the calculations based on Eqs. (15)–(17) are given.

Well Size $L$ (Å)	(110) QW's						(113) QW's					
	(Ref. 1)	$\delta_{hh}$ (Ref. 4)	$\delta_{hh}$ (Ref. 8)	$\delta_{hh}$ Cal.	$\delta_{lh}$ (Ref. 8)	$\delta_{lh}$ Cal.	$\delta_{hh}$ (Ref. 8) <sup>†</sup>	$\delta_{lh}$ (Ref. 8) <sup>†</sup>	$\delta_{hh}$ (Ref. 5)	$\delta_{hh}$ Cal.	$\delta_{lh}$ (Ref. 5)	$\delta_{lh}$ Cal.
200			0.2	0.17	-0.38	-0.34	0.19	-0.39				
90		0.2	0.26	0.23	-0.4	-0.4	0.3	-0.42				
65			0.34	0.3	-0.46	-0.45	0.43	-0.45	-0.07	-0.07	0.1	0.15
54			0.39	0.38	-0.49	-0.47	0.52	-0.5	-0.09	-0.09	0.12	0.16
47			0.46	0.42	-0.53	-0.5	0.64	-0.55	-0.11	-0.1	0.13	0.17
40	0.42		0.5	0.45	-0.61	-0.53	0.79	-0.58				
35			0.56	0.64	-0.69	-0.57	0.9	-0.64	-0.21	-0.16	0.25	0.21

corrections decreases. In that way, our calculations overestimate the values of the anisotropy compared to the real model of the finite potential barrier QW's. Apparently, it follows from this that the optical anisotropy is larger in QW's with high potential barrier. By using Eqs. (15), the relative optical anisotropy in dependence of the well thickness was calculated for the [110]-oriented GaAs and AlAs QW's. The following values of the band parameters were used:  $\gamma_2=2.1$ ,  $\gamma_3=2.9$ ,  $\Delta_{so}=340$  meV, for GaAs and  $\gamma_2=0.78$ ,  $\gamma_3=1.57$ ,  $\Delta_{so}=280$  meV, for AlAs. Figure 2 shows the plot of the functions  $\gamma_{lh}=\delta_{lh}+1$  and  $\gamma_{hh}=\delta_{hh}+1$  vs the well thickness  $L$  for GaAs QW's [Fig. 2(a)] and for AlAs QW's [Fig. 2(b)].

One can see that the anisotropy of the optical matrix elements reaches significant values, e.g., in the AlAs QW at  $L=50$  Å, the probability of the 1hh-1c direct optical transition when the light wave is polarized along the axis (1 $\bar{1}$ 0) is 1.5 times larger than that of the wave polarized along the axis (001). On the contrary, the optical matrix elements of the 1lh-1c transition is three times smaller for the former polarization direction than for the latter.

(v) In conclusion, we give the comparison of the analytic results with the experimental data. The in-plane polarization dependence of the optical spectra was observed in the GaAs/AlAs QW's systems. In Refs. 1 and 4 the [110]-oriented QW's were studied, while in Ref. 5 the [113]-oriented QW's were investigated. The numerical calculations of the quantities  $\delta_{lh, hh}$  in [110]-oriented QW's were performed by Nojima [Ref. 8 (1993)]. The experimental data by Gershoni *et al.*,<sup>1</sup> Kajikawa *et al.*,<sup>4</sup> Belousov *et al.*,<sup>5</sup> as well as our calculations on the  $\delta_{lh}$  and  $\delta_{hh}$  are given in Table I. It may be seen from Table I that our results are in good agreement with the experimental data by Gershoni *et al.*<sup>1</sup> and Kajikawa *et al.*,<sup>4</sup> also shown in Fig. 2. They are also in agreement with the experimental results by Belousov *et al.*,<sup>5</sup> especially for the quantities  $\delta_{hh}$  (at the well thickness larger than  $\sim 50$  Å). However, the computed values  $\delta_{lh}$  are slightly larger than

the measured ones. Perhaps, the experimental data are underestimated since the heavy-hole continuum overlaps with the light-hole exciton peak. Our results are in agreement with the numerical calculations by Nojima<sup>8</sup> for the well thickness larger than  $\sim 50$  Å, with the exception of the data on the  $\delta_{hh}$  in GaAs/AlAs QW's.

#### IV. CONCLUSIONS

In this paper, the Luttinger-Kohn effective mass theory has been used to calculate the interband optical transitions in (11 $N$ )-oriented QW's. In (11 $N$ )-,  $N \neq 1$ , oriented QW's the interband matrix elements are anisotropic. The optical anisotropy is caused by the nonanalyticity of the hole wave functions in the vicinity of the point  $\vec{k}_1=0$ . The intrinsic optical anisotropy is the more pronounced, the stronger the anisotropy of hole effective masses and the higher the potential barrier of the quantum well.

Our results enable one to compute exactly the minimum values of the relative optical anisotropy. It is shown also that the mixing of the  $\Gamma_8$  and  $\Gamma_7$  states leads to a dependence of the effect on the QW's thickness. For relatively wide QW's, this mixing can be treated as a perturbation. In this case, the optical anisotropy in finitely high potential barrier QW's increases with decreasing well thickness as  $1/L^2$ . Note, also, that the anisotropy of the optical matrix elements leads to the intrinsic anisotropic optical effects in quantum wells, such as anisotropic absorption and reflection spectra, as well as the natural birefringence.

#### ACKNOWLEDGMENTS

This work has been supported by the Deutsche Forschungsgemeinschaft. I am thankful to Professor Dr. Arkadii Aronov (Rehovot) and to Dr. C. Klingshirn (Karlsruhe) for helpful discussions.

\*Permanent address: Institute of Cybernetics, Academy of Sciences of Georgia, Euli 5, 380086 Tbilisi, Georgia.

<sup>1</sup>D. Gershoni, I. Brener, G. A. Baraff, S. N. G. Chu, L. N. Pfeiffer, and K. West, Phys. Rev. B **44**, 1930 (1991).

<sup>2</sup>R. Notzel, N. N. Ledentsov, L. Dawezitz, H. Hobenstein, and K. Ploog, Phys. Rev. Lett. **67**, 3812 (1991).

<sup>3</sup>R. Notzel, N. N. Ledentsov, and K. Ploog, Phys. Rev. B **47**, 1299 (1993).

- <sup>4</sup>Y. Kajikawa, M. Hata, T. Isu, and Y. Katayama, *Surf. Phys.* **267**, 501 (1993).
- <sup>5</sup>M. V. Belousov, V. L. Berkovits, A. O. Gusev, E. L. Ivchenko, P. S. Kopev, N. N. Ledentsov, and A. S. Nesvizhskii, *Fiz. Tverd. Tela (St. Petersburg)* **36**, 1098 (1994) [*Phys. Solid State* **36**, 596 (1994)].
- <sup>6</sup>It is known that bulk cubic crystals exhibit natural optical anisotropy due to the spatial dispersion of light; see V. M. Agranovich and V. L. Ginsburg, *Spatial Dispersion in Crystal Optics and the Theory of Excitons* (Nauka, Moscow, 1979).
- <sup>7</sup>N. Peyghambarian, S. W. Koch, and A. Mysyrowicz, *Introduction to Semiconductor Optics* (Prentice-Hall, Englewood Cliffs, NJ, 1993).
- <sup>8</sup>S. Nojima, *Phys. Rev. B* **47**, 13 535 (1993); *Jpn. J. Appl. Phys.* **31**, 2765 (1992); **31**, L1401 (1992).
- <sup>9</sup>J. M. Luttinger and W. Kohn, *Phys. Rev.* **97**, 869 (1955).
- <sup>10</sup>L. Lowdin, *J. Chem. Phys.* **19**, 1396 (1951).
- <sup>11</sup>Note, that these conditions are realistic. Even in QW's with a well thickness of only  $L = 50 \text{ \AA}$  the quantization energy  $\epsilon_q = \hbar^2 \pi^2 / 2m_0 L^2 \approx 15 \text{ meV}$ . On the other hand, the spin-orbit splitting  $\Delta_{so}$  is usually of the order of 100 meV, i.e., larger than  $\epsilon_q$ . For example,  $\Delta_{so} = 340 \text{ meV}$  in GaAs. As to the potential barrier, it can be very different in the various QW's. Nevertheless, in many experimentally studied QW's, the potential barrier is sufficiently high. For example, the offsets of the valence band and conduction band are  $\sim 150$  and  $\sim 250 \text{ meV}$ , respectively, for GaAs/ $\text{Al}_{0.3}\text{Ga}_{0.7}\text{As}$  QW's, and those are  $\sim 400$  and  $800 \text{ meV}$  for GaAs/AlAs QW's.
- <sup>12</sup>Y. Kajikawa, M. Hata, and T. Isu, *Jpn. J. Appl. Phys.* **30**, 1944 (1991).
- <sup>13</sup>See, e.g., E. G. Tsitsishvili, O. V. Gogolin, J. L. Deiss, and V. N. Bagdavadze, *Solid State Commun.* **56**, 717 (1985), and references therein.
- <sup>14</sup>Note, that as usual, the band parameters  $\gamma_2$  and  $\gamma_3$  are close to each other. In this case, the functions  $\gamma_{\pm}(\chi)$  in Eq. (17) are positive at any angle  $\chi$ . In the particular case of  $\gamma_2 \approx \gamma_3 \approx \bar{\gamma}$ ,  $\gamma_+ \approx \bar{\gamma}$ , and  $\gamma_- \approx 3\bar{\gamma}$ .
- <sup>15</sup>It may be assumed that the excitonic and interband transitions have the same anisotropy, since the corresponding states are constructed from the same wave functions.